Weak transverse field μSR measurements as an experimental probe of magnetic materials

Megan R. Rutherford
University of British Columbia
Physics and Astronomy
(Dated: December 14, 2021)

Weak transverse field (wTF) muon spin relaxation measurements are a type of μSR experiment in which a very weak external magnetic field is applied perpendicular to the initial polarization of the muon spin. Weak transverse field experiments are often used to determine fitting parameters used in the analysis of other μSR experiments. However, wTF μSR also can act as a tool to measure the partial volume fraction of a magnetic material as a function of pressure or temperature. A description of this technique, as well as some examples of studies in which these measurements have proved fruitful, are discussed.

I. INTRODUCTION TO μSR

Weak transverse field muon spin relaxation (wTF μSR) experiments are a very powerful tool in the study of certain magnetic materials. Before discussing these measurements in detail, a background describing the μSR technique in general will be provided. In 1974 Toshi Yamazaki, Ken Nagamine, Ken Crowe, and Jess Brewer coined the term μSR to describe the experimental technique of studying the interactions of the muon spin via the asymmetry of the particle's decay. The acronym stands for "**M**uon **S**pin **R**elaxation, **R**otation, **R**esonance, **R**easearch or you" [1]. In the years following, this large scale facility technique has become a powerful local probe of weak internal magnetic fields present within condensed matter systems.

A. Muon Production

A muon is an electron-like lepton (a charged, spin $\frac{1}{2}$ subatomic particle that does not undergo strong interactions) with an average lifetime of 2.2 μs. Muons exist ambiently, primarily in the upper atmosphere where cosmic rays interact with gas particles. However, to achieve the flux of muons required to perform statistically significant analysis, we must produce them artificially.

There exist several different techniques by which this artificial production of muons is accomplished, which are expanded upon in references [2–4]. Henceforth, the experimental details in this section are relevant to those used at TRIUMF in Vancouver located on UBC campus. There, H^- ions are injected into a large cyclotron and are accelerated to 500 MeV. A carbon foil is used to strip the electrons leaving behind high energy protons that are directed towards a low Z-number (in this case beryllium) target. When protons collide with the target, pions are produced. Positively charged pions have a lifetime of approximately 26 ns and then decay via the following process:

$$\pi^+ \longrightarrow \mu^+ + \nu_\mu. \quad (1)$$

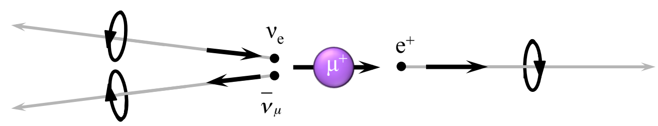

Figure 1. The decay of a muon into a positron, and two neutrinos. Black arrows show the momentum and handedness of each decay particle, while grey arrows show the direction of travel of each particle.

Low energy pions with insufficient energy to escape the beryllium target are considered to be at rest, and are referred to as surface pions, which produce muons that are 100% spin polarized and have a kinetic energy of 4.119 MeV [1] in the rest frame of the pion. Note that all pions used in the production of muons at TRIUMF are positive, and therefore produce positive muons.

Once muons are produced, dipole magnets are used to select muon momentum, and quadrupole magnets are used to focus the muon beam and direct the muons towards the sample environment. The muon is a local probe, and therefore it must be implanted into the sample such that it penetrates deeply enough into the material that it interacts with the local environment, though not so deep that it passes through.

B. Muon implantation and decay

Once the muon is implanted into the sample, the muon will spontaneously decay into a positron. This positron is preferentially emitted along the initial direction of the muon spin at the time of decay (as seen in Figure 1).

The positron and two neutrinos are emitted according to the decay pathway:

$$\mu^+ \longrightarrow e^+ + \overline{\nu}_\mu + \nu_e. \quad (2)$$

This process is a three-body final state decay, which means that, the resulting positron will not have an exact energy or momentum but rather a distribution of energies and momenta. The positron is emitted preferentially

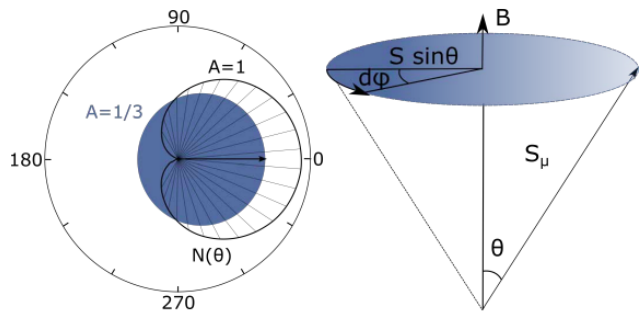

Figure 2. The image on the left shows the angular distribution of positrons that result from the decay of a muon, given in equation 3 above. The asymmetry parameter a=1/3 when all positron energies are sampled with equal probability [4]. On the left is the Larmor precession of the muon's spin around a local magnetic field. Figure taken from [5]

along the direction in which the muon spin was oriented at the time of decay. However, they are not emitted precisely along the muon spin direction. The following probability function gives the distribution of emission directions:

$$N(\theta) = 1 + A\cos(\theta), \tag{3}$$

where θ is the angle between the muon spin and direction of positron emission, and A is the asymmetry factor that increases monotonically with the positron energy. The value of $A = 1$ gives a maxiumum energy of 52.83 MeV. The average value of $A = \frac{1}{3}$. How the angular probability distribution function $N(\theta)$ varies can be seen in Figure 2 [1].

Since the muon is a spin-1/2 particle, once it comes to rest within the material, its magnetic moment will precess in the local magnetic environment with a frequency of $\omega_\mu = \gamma_\mu B_{loc}$ (where γ_μ is the gyromagnetic ratio of the muon, and B_{loc} is the local magnetic field that is experienced by the muon). The spin direction of the muon will evolve within the sample, and the extent of this precession is revealed in the counting rates of the detectors. Unlike the neutrinos that are produced, the emitted positron can be easily detected via a scintillation detector. The detectors are attached to photomultipliers which are used to give statistics on the precession of the muon as a function of time. Detector counting rates are combined and measure a decay spectrum of the muon lifetime, which forms an asymmetry plot that is proportional to the spin polarization function. This polarization function is given by the ensemble average of the probability that a positron will be detected by a specific counter. This depends on several variables including the asymmetric muon decay pattern, the direction of the muon spin at the time of decay, and the position and shape of the counter.

As we are measuring a decay spectrum that pertains to the muon lifetime, it is essential that the decay event is due to a known muon (i.e. that this process is electronically gated to prevent ambiguity between the decay of multiple muons). This comes from the fact that the statistics of our measurement and the precession are both time dependent. This allows us to match a decay event to a specific muon, giving confidence in the polarization function that is extracted.

Analysis of this polarization function requires special consideration of the experimental geometry, as discussed in the following section.

II. EXPERIMENTAL GEOMETRY

Muon spin relaxation, rotation, and resonance experiments yield data that can be analyzed in a number of ways, for the purposes of this paper, the relevant classification of experimental geometries are those of longitudinal (LF)/zero (ZF) field, and transverse (TF)/weak transverse (wTF) field. The distinction between the two geometries is solely in the relative direction of the initial muon polarization in comparison to that of an externally applied magnetic field. The focus of this work is the subset of experiments involving the wTF orientation, however it is relevant for context to briefly describe each of them.

Longitudinal and zero field μSR experiments consider the time evolution of the muon polarization where there is an external magnetic field applied parallel to said polarization. Zero field measurements are thought of as LF measurements in the zero field limit. It is a special feature of muons that they can probe the zero field relaxation of materials. This is in contrast to NMR or ESR (electron spin rotation) techniques (which are in some ways analogous to μSR). As previously stated, longitudinal relaxation of the signal is completely due to time-dependent interactions taking place within the material [2]. This makes this type of measurement well suited for probing physical properties of bulk materials that are a result of the recovery of thermodynamic equilibrium. These experiments are typically performed to investigate materials in which the magnetism is static, or in which the magnetism is dynamically fluctuating [6].

Unlike for LF measurements, a signal that results from TF μSR describes relaxation processes that are unrelated to energy loss such as spin-spin interactions, etc. Here the external magnetic field is applied transverse to that of the initial muon polarization. This is accomplished by rotating the muon spin so that is is oriented perpendicular to the direction - referred to as "spin rotate mode." This technique is widely used to determination of local magnetic susceptibility, or the field distribution in inhomogeneous samples [7].

During a μSR experiment, the detector orientation, the applied magnetic field, and muon spin orientation are all variables over which the experimenter has some amount of control. As such there exists a labelling convention that has been devised to describe μSR experiments using surface muons (that are initially spin polarized antipar-

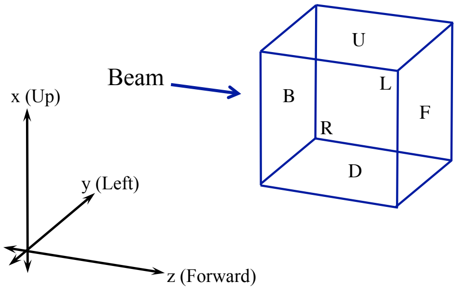

Figure 3. The coordinate system conventionally used in μSR experiments to label each of the six different detectors relative to the incoming muon beam.

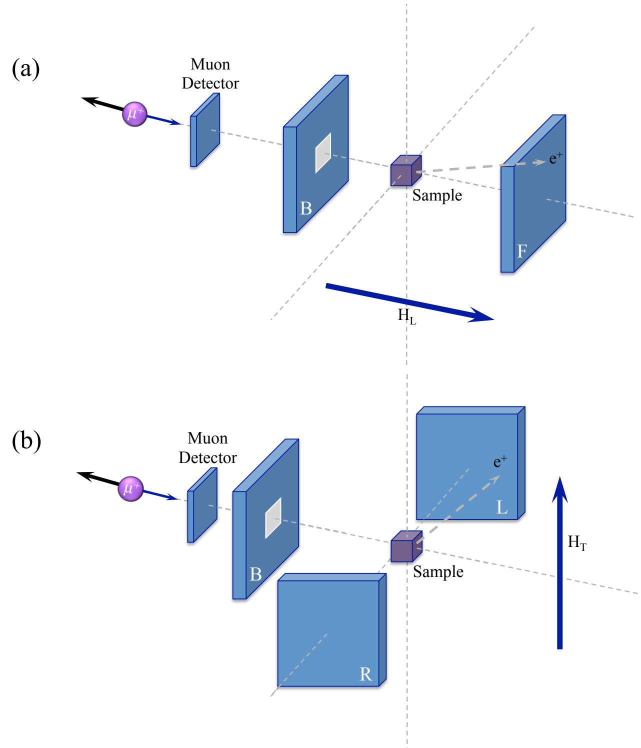

Figure 4. Geometry of the positron detectors surrounding the sample for (a) a longitudinal field muon relaxation measurement, and (b) a transverse field muon experiment. The muon detector triggers a timer to measure the time between muon implantation and decay, forward and backwards detectors are used to detect positron emission. The blue arrow indicates the trajectory of the muon and the black arrow indicates the spin of the muon. Figure adapted from [8].

allel to their momentum vector). The standard array of scintillation detectors consists of six counters which are oriented as seen in Figure 3. They are labelled F (forward), B (backward), U (up), D (down), L (left), and R (right). The unrotated implanted muon polarization points towards the backward counter. A schematic of the relative position of the sample and detectors is shown in Figure 4 for both the longitudinal, and transverse applied magnetic field orientations.

A. Derivation and Interpretation of Asymmetry

The μSR asymmetry spectra can be extracted from the time histogrammed decay positron spectra. The number of decay positrons, $N_i(t)$, can be determined according to the equation below:

$$N_i(t) = N_i^0 e^{-t/\tau_\mu}[1 + A_i^0 P_i(t)] + B_i^0, \tag{4}$$

where N_i^0 is a normalization constant and A_i is the maximum precession amplitude (the intrinsic asymmetry of the positron detector). B_i^0 is a time independent random background that results from spurious "stop" signals detected by the positron detectors that do not correspond to the decay of the muon within the sample, and $P_i(t)$ is the time evolution of the muon spin polarization. The polarization function, $P_i(t)$, is given by:

$$P_i(t) = \cos(\omega_\mu t + \theta_i), \tag{5}$$

where ω_μ is the precession frequency of the muon and θ_i is the initial phase of the muon spin polarization vector.

Equation 4 can be applied to each counter in the forward-backward pair and the counts can be combined to obtain a total asymmetry function as follows:

$$N_F(t) = N_F^0 e^{-t/\tau_\mu}[1 + A_F^0 P_z(t)], \tag{6}$$

$$N_B(t) = N_B^0 e^{-t/\tau_\mu}[1 - A_B^0 P_z(t)], \tag{7}$$

$$A_F P_z(t) = \frac{\alpha N_F(t) - N_B(t)}{\alpha\beta N_F(t) + N_B(t)}, \tag{8}$$

where $\alpha = \frac{N_B^0}{N_F^0}$, and $\beta = \frac{A_B}{A_F}$. In this context, α is a parameter that corrects for the differences in the solid angle of opposing detectors, as well as difference in efficiency, beam intensity, and delivery. The β parameter corrects for the difference in counter asymmetry based off of the construction of the counters. Changes in α are seen in the asymmetry spectra as y-offset, whereas changes in β result in a distortion of the vertical axis. While β is generally expected to be close to 1. Unlike α which is obtained from a universal fit to transverse field data measured in a weak field (≈2-4 mT) [2].

B. Weak transverse field measurements

A subset of transverse field measurements referred to as "weak transverse field," or wTF measurements are performed in non-spin rotate mode, but with a weak external magnetic field applied transversely to the direction of the muon spin. Since the response should be approximately that of a non-relaxing, and non-precessing state when a weak transverse field is applied to a paramagnetic sample. These measurements are often done several times during every μSR experiment, as a means to determine the value of the α parameter. This parameter corrects for the differences in the solid angle of opposing detectors, as well as differences in efficiency, beam intensity, and muon delivery. As mentioned in Section II A, this is extracted from transverse field spectra that oscillate symmetrically about the time axis [2].

More relevant to the remainder of this paper, is the use of weak magnetic field μSR measurements to investigate materials with partial ordering. The amplitude of the measured signal is proportional to the volume fraction of that phase. This is an incredibly useful property of this type of measurement as it implies that small impurity phases do not effect the muons. Muons implanted in an ordered regime will decouple, resulting in a a rapid relaxation described by an exponential component, and muons in the non-ordered regime will precess slowly, as they would in straightforward paramagnetic materials (outlined above). The asymmetry function will then describe both of these regimes if it is given the following form:

$$A_0 P(t) = A_{para} \mathrm{e}^{-\lambda_{para} t} \cos(\omega_{mu} t + \phi) + A_{fast} \mathrm{e}^{-\lambda_{fast} t}, \tag{9}$$

where A_0 is the initial asymmetry, *P(t)* is the muon polarization function, ω_μ is the Larmor frequency, ϕ is the initial phase of the precession, and A_i and $_i$ (i = *para, fast* are the asymmetries and exponential relaxation rates of the two signals that arise from the separate phases present within the sample [9]. The resulting data set can be fit to a function of this form, relative asymmetry values will give us the ordered volume fraction of the sample. There are many examples of this type of measurement being used in the investigation of magnetic materials throughout the literature. A selection of these will be discussed further in section III.

III. APPLICATIONS

In comparison to LF and TF μSR, wTF measurements are less widely used. However, this type of measurement has been instrumental in providing tangible evidence for various quantum phenomena occurring within a wide range of condensed matter systems. Particularly in cases where there are phenomenological differences in certain sample volumes that develop as a function of temperature or pressure.

In μSR studies of thin films, with samples on the order of microns - millimetres thick, a much greater portion of the muon beam penetratecs through the sample. This increases the likelihood of incorrectly interpreting the relaxation function. Weak transverse field measurements are used in order to resolve which fraction of the asymmetry signal comes from the actual sample, and which comes from the sample holder [10, 11]. In studies of magnetic systems that exhibit multi-phased ground states, wTF measurements are very useful for determining the nature and volume of these various regimes of magnetic behaviour [12, 13]. Weak transverse field measurements are also used to determine the existence and nature of magnetic phase separation [14]. They can be used to investigate the coexistence of long and short ranged magnetic order [15, 16], as well as to study magnetic phase transitions [9, 17, 18]. The small size of the applied magnetic field is also well suited to the study of systems with fragile ground states, namely those which exhibit geometric frustration [19]. There have also been several studies using wTF μSR to Li^+ ion diffusion in potential positive cathode materials [20, 21] by tracking the development of localized moments within the material as a function of temperature.

Two different studies in which wTF measurements were crucial to the final interpretation of the data will be expanded upon in more detail in the remainder of this section. This is meant to provide a complete picture illustrating how wTF μSR can contribute to our physical understanding of quantum materials.

A. Probing the quantum phase transition of Mott insulators

The study of $RENiO_3$ (RE = rare earth element) by Frandsen *et al.* [22], used wTF μSR to investigate the volume-wise destruction of the Mott insulating state near the quantum phase transition. The $RENiO_3$ class of materials are considered to be one of the archetypal examples of Mott insulators, which can be tuned via systematic variation of the rare-earth ion and as such it is an excellent system in which to study quantum phase transitions (QPT). Previous to this study, the order of this phase transition was unknown. Whether a QPT is first- or second-order is significant as a second-order transition leads to quantum criticallity that could possibly result in exotic phenomena.

Frandsen and collegues used μSR to measure the local order parameter and magnetically ordered volume fraction independently. As seen in the experimental results (seen in Figure 5), the QPT from a paramagnetic metal to an antiferromagnetic insulator is first order. In particular, the wTF measurements where used to plot the behaviour of the magnetically ordered volume fraction which heavily decreases until it reaches zero at the QPT. The wTF asymmetry spectra were modelled using the following function:

$$A(t) = a_p \exp(-\Lambda t) \cos(\omega t + \phi), \tag{10}$$

where A(t) is the time-dependent asymmetry, a_p is the amplitude of the oscillating component (related to

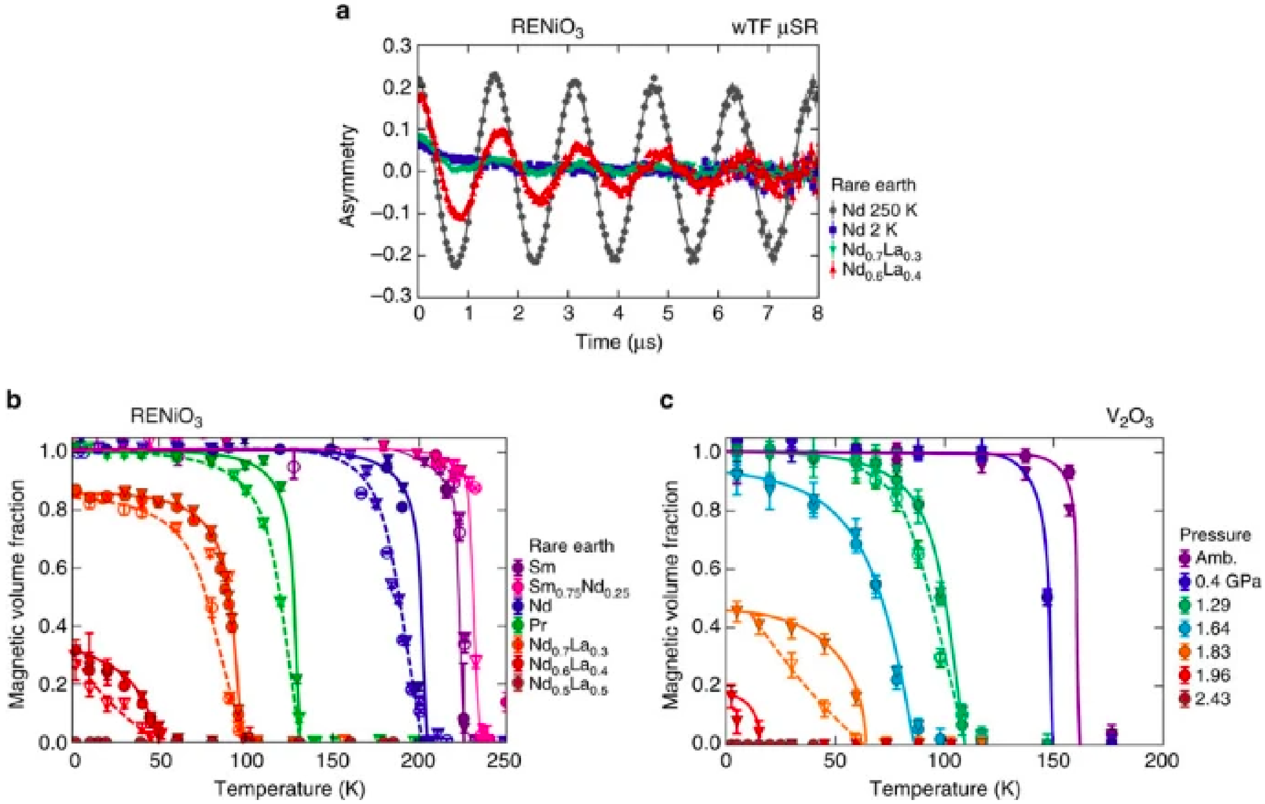

Figure 5. **(a)** wTF time spectra for three compound in the $RENiO_3$ family that lie near the QFT. **(b)** The temperature dependence of the magnetic volume fraction in $RENiO_3$ derived from fitting the wTF data. Compounds near the QPT have a significantly reduced magnetic volume fraction near the QPT. **(c)** Analogous magnetic volume fraction data for V_2O_3 shown as a sanity check that this behaviour is related to the Mott insulating QPT. Figure from [22].

the paramagnetic volume fraction), Λ is an exponential damping rate, ω is the Larmor precession frequency, and ϕ is a phase constant. As described in Section II B, the QPT is tracked by seeing how the partial ordering from paramagnetic to antiferromagnetic is affected by temperature. The "fast" component of the asymmetry remains small about T_N, but becomes smaller with a decrease in temperature down to base temperature (as can be seen in Figure 5, panel **b**. This data, particularly where the magnetic volume fraction approaches zero in every member of the series, was instrumental in determining that this phase transition is first order [22].

B. The coexistence of superconductivity and magnetism

The discovery of FeAs-based superconductors provided a further opportunity to investigate the mechanism of superconductivity in correlated electron systems. Unlike the cuprates, this class of materials exhibit coexisting static magnetism and superconductivity. One of the issues addressed by Aczel *et al.* in 2009 [23], and Goko *et al.* in 2009 [24] was the interplay between superconductivity and magnetism.

Muon spin relaxation measurements showed that for AFe_2As_2 (A = Ca, Ba, Sr), superconductivity coexists with a strong static magnetic order in a partial volume fraction of the material. These wTF measurements can be seen in the centre panel of Figure 6.

Once again, the authors performed wTF μSR measurements in order to obtain the volume fraction of the material which was paramagnetic and which was not. This can illuminate how the superconductivity in these materials coexist with magnetism as we see how this volume fraction changes over a range of temperaures.

IV. CONCLUSION

Muon spin relaxation is a technique that has been widely used in the investigation of strongly correlated electronic materials over the past several decades. Muons are produced in enough abundance that, when they are implanted into a material and allowed to decay, information can be garnered about the local environment in which the decay occurred. Weak transverse field (wTF) μSR measurements are a type of measurement in which

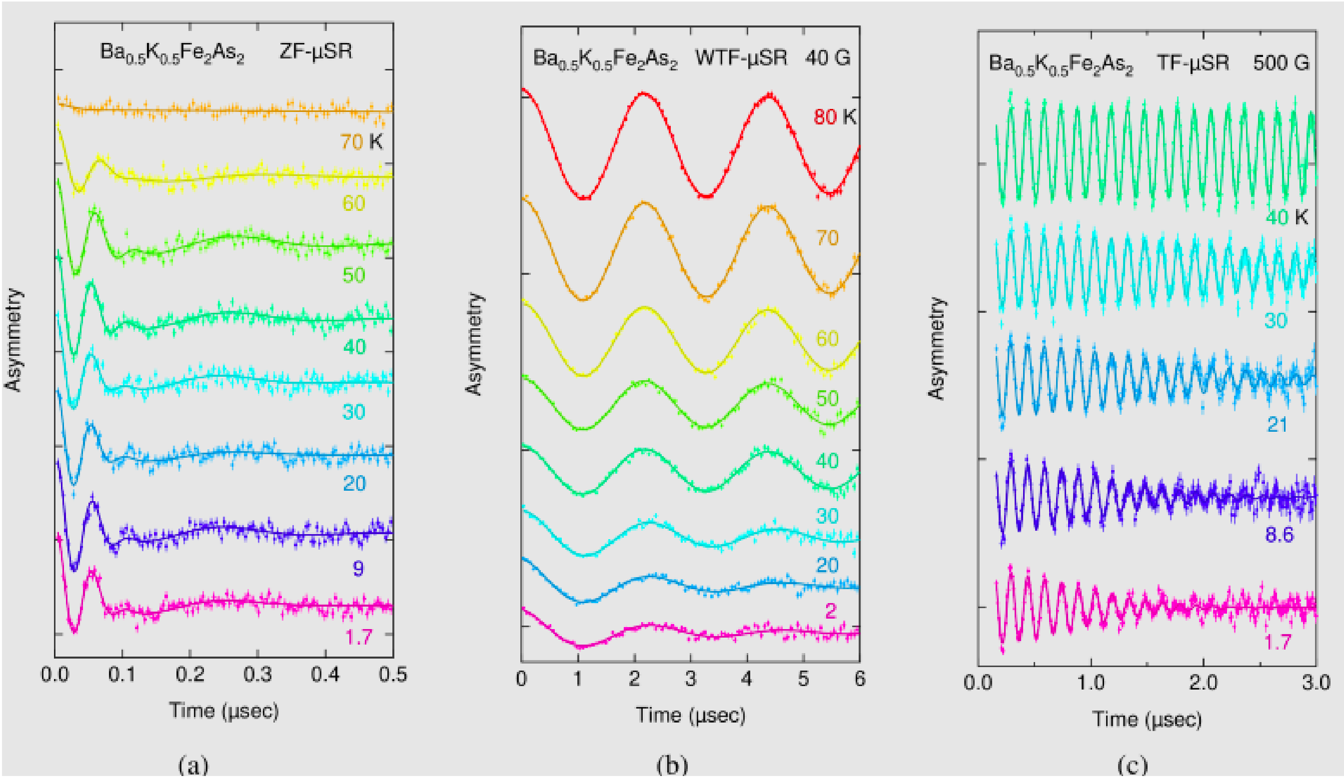

Figure 6. This figure provides a nice example of what data from each of the different experimental geometries can be expected to look like **(a)** zerofield μSR **(b)** weak-transverse field μSR **(c)** transverse field μSR. All measurements depicted were performed on a single crystal of $Ba_{0.5}K_{0.5}Fe_2AsF_2$. Figure from [24].

a very weak external magnetic field is applied perpendicular to the initial polarization of the muon spin. While these measurements are usually performed to extract parameters used in the analysis data acquired in other μSR measurements, wTF measurements are useful in their own right. Weak transverse field data can be fit using compound functions which allow for the resolution of magnetic behaviour that occurs over some partial volume of the material. The ability to measure the partial volume fraction as a function of pressure or temperature is incredibly useful in the study of magnetic transitions, multi-phase ground states, etc. In particular, the volume-wise destruction of the Mott insulating state, and the co-existence of superconductivity and magnetism in FeAs-based superconductors are discussed in some detail.

[1] J. H. Brewer and R. Cywinski, usr: an introduction, in *Muon Science: Muons in Physics, Chemistry and Materials*, Proceedings of the Fifty First Scottish Universities Summer School in Physics, edited by S. L. Lee, S. H. Kilcoyne, and R. Cywinski (Taylor Francis and Group, 1998).

[2] G. H. Eaton and S. H. Kilcoyne, Muon production: past, present, and future, in *Muon Science: Muons in Physics, Chemistry and Materials*, Proceedings of the Fifty First Scottish Universities Summer School in Physics, edited by S. L. Lee, S. H. Kilcoyne, and R. Cywinski (Taylor Francis and Group, 1998).

[3] P. D. de Reotier and A. Yaouanc, Muon spin rotation and relaxation in magnetic materials, Journal of Physics: Condensed Matter **9** (1997).

[4] J. E. Sonier, Muon spin muon spin rotation/relaxation/resonance (µsr) (2002).

[5] K. Papadopoulos, *Investigation of magnetic order in nickel- 5d transition metal systems*, Ph.D. thesis, Uppsala University (2019).

[6] S. J. Blundell, Spin-polarized muons in condensed matter physics, (1999).

[7] Sonier, msr studies of the vortex state in type-ii superconductors, (2000).

[8] M. R. Rutherford, *Dy2ScNbO7: a study of the effect of a disorderedB-site on the spinice magnetism typically seen in dysprosium pyrochlores*, Ph.D. thesis, McMaster University (2021).

[9] Russo, Muon spin rotation and relaxation study of ba2coo4, (2009).

[10] M. Bator, Y. Hu, H. Luetkens, C. Niedermayer, T. Prokscha, A. Suter, Z. Salman, M. Kenzelmann, C. W. Schneider, and T. Lippert, Depth-dependent spin dynamics in tbmno3 thin fils measured by low energy muon spin

relaxation, Physics Procedia **30**, 137 (2021).

[11] R. F. Need, Quasistatic antiferromagnetism in the quantum wells of smtio3/srtio3 heterostructures, NPJ (2018).

[12] O. K. Forslund, Intertwinded magnetic sublattices in the double perovskite compound lasrnireo$_6$, .

[13] Z. GUGUCHIA, Magnetism in semiconducting molybdenum dichalcogenides, (2018).

[14] M. Mitschek, T. Hicken, S. Yang, M. N. Wilson, F. L. Pratt, C. Wand, S. J. Blundell, Z. LI, Y. Li, T. Lancaster, and J. M, Probing the magnetic polaron state in the ferromagnetic semiconductro hgcr$_2$se$_4$ with resistance fluctuation and muon-spin spectroscopy measurements, The ArXiv.

[15] Khatua, Development of short and long-range magnetic order in the double perovskite based frustrated triangular lattice antiferromagnet ba[formula: see text]mnteo[formula: see text]. development of short and long-range magnetic order in the double perovskite based frustrated triangular lattice antiferromagnet ba[formula: see text]mnteo[formula: see text]., (2021).

[16] R. Akiyama, Short range spin correlations in b-lifeo2 from bulk magnetization, neutron diffraction and musr experiments, Physical Review B (2010).

[17] J. Sugiyama, Comparative muon-spin rotation and relaxation study on the zigzag chain compounds namn2o4 and li0.92mn2o4, (2009).

[18] M. Mansson, Magnetic order and transitions in the spin-web compound cu3teo6, (2012).

[19] J. Sugiyama, Magnetism of layered cobalt oxides investigated by muon spin rotation and relaxation, PRB (2002).

[20] J. Sugiyama, Low-temperature magnetic properties and high-temperature diffusive behaviour of linio$_2$ investigated by muon-spin spectroscopy, (2010).

[21] K. Mukai, Magnetism and lithium diffusion in li$_x$coo$_2$ by a muon-spin rotation and relaxation (μ^+sr) technique, Journal of Power Sources **174** (2007).

[22] B. A. Frandsen, L. Liu, S. Cheung, Z. Guguchia, R. Khasanove, E. Morenzoni, T. J. S. M. Munsie, and A. H, Volume-wise destruction of the antiferromagnetic mott insulator state through quantum tuning, (2016).

[23] A. A. Aczel, Muon spin relaxation studies of magnetic order and superfluid density in antiferromagnetic ndofeas, bafe 2 as 2 and superconducting (ba,k)fe 2 asmuon spin relaxation studies of magnetic order and superfluid density in antiferromagnetic ndofeas, bafe 2 as 2 and superconducting (ba,k)fe 2 as, ArXiv (2008).

[24] T. Goka, Superconductivity coexisting with phase-separated static magnetic order in (ba, k)fe2as2, (sr, na)fe2as2, cafe2as2 - cite axcel and sonier in this section, PRB (2009).